MENU 2007
11th International Conference
on Meson-Nucleon Physics and
the Structure of the Nucleon
September10-14, 2007
IKP, Forschungzentrum Jülich, Germany

NUCLEON AND PION-NUCLEON FORM FACTORS FROM LATTICE QCD

A. Tsapalis [1]
Institute of Accelerating Systems and Applications, University of Athens
Athens, Greece

Abstract

The isovector Nucleon electromagnetic form factors $G_E(q^2)$ and $G_M(q^2)$ are evaluated in Lattice QCD using Wilson fermions. A lattice of spatial extent 3 fm is used in the quenched theory allowing the extraction of the form factors for momentum transfer squared between 0.1 and 2 GeV^2 for lowest pion mass of about 400 MeV. The calculation is also performed using two degenerate dynamical flavors of Wilson quarks for pion masses comparable to those in the quenched theory allowing a direct comparison. An effective chiral theory is used for the extrapolation of the magnetic moment and isovector radii at the physical limit.

In addition, we present recent results from the calculation of the momentum dependence of the axial form factors $G_A(q^2)$ and $G_p(q^2)$ along with the calculation of the $G_{\pi NN}$ form factor on the same set of lattices. This enables us to test the Goldberger-Treiman relation and compare to the experimental value of the pion-nucleon strong coupling constant $g_{\pi NN}$.

1 Introduction

Form factors maintain a central role in the study of hadron structure. They yield information on the size, magnetization and charge distribution in hadrons. They are functions of the Lorentz invariant momentum transfer squared probing the interaction of a hadron with a current. The electromagnetic structure of the nucleon is probed by the coupling of a photon with a quark, a process parameterized by the electric, G_E, and the magnetic, G_M form factor. A photon exchanging momentum $\vec{q}$ probes a length scale of roughly $1/|\vec{q}|$ and therefore a range of momentum transfers is required in order to map the full spatial distribution. The traditional picture of the nucleon electric and magnetic form factors having similar q^2 dependence based

[1] Invited speaker at the Conference

on data using Rosenbluth separation has been revised recently by precise polarization measurements [1], which indicate an approximately linear q^2 dependence of the ratio of $G_E(q^2)/G_M(q^2)$.

Lattice QCD enables a non-perturbative study of these fundamental quantities using directly the fundamental theory of strong interactions. State-of-the-art lattice calculations can reach pion masses as low as 350 MeV where chiral effective theories begin to be applicable. Having reliable predictions from chiral theories on the dependence of physical quantities on the pion mass [2, 3] provides the bridge connecting lattice results to experiment.

The exchange of a W or Z boson probes different dynamics inside the nucleon. Two additional form factors enter, namely the axial-vector $G_A(q^2)$ and the induced pseudoscalar $G_p(q^2)$. Chiral symmetry breaking and the associated partial conservation of the axial current (PCAC) constrains the behavior of these form factors. Pion pole dominance is directly reflected in the q^2-dependence of G_p while both form factors are related to the pseudoscalar nucleon form factor, $G_{\pi NN}(q^2)$, defined through the pion-nucleon vertex. Quasi-elastic neutrino scattering [4] and pion electroproduction experiments [5, 6] are consistent with a dipole q^2-dependence for G_A up to $1\,\mathrm{GeV}^2$. G_p is less well known, with muon capture experiments [7] being the main source of measurements of $G_p(-0.88m_\mu^2)$ and pion electroproduction probing the q^2 dependence. At small q^2 [6] the data are well represented with a dipole *Ansatz*. In this work we present the calculation of the isovector nucleon electromagnetic form factors [8] in quenched QCD and using two degenerate flavors of dynamical Wilson fermions. Optimal techniques are employed allowing the evaluation on a large range of momenta with reduced statistical error. In addition we evaluate the axial-vector form factors and the $\pi - N$ pseudoscalar form factor [9] for a range of momenta transfers up to $2\,\mathrm{GeV}^2$, which allows us to examine the validity of pion dominance and the associated Goldberger-Treiman (GT) relation. Recent studies of these quantities in Lattice QCD with dynamical quarks using different discretizations [10, 11] yield comparable results to ours. Consistency among the different approaches is indicative that lattice artifacts are under control.

It is worth mentioning that additional information on the nucleon structure is contained in the transition form factors of the nucleon to the $\Delta(1232)$ resonance. Recent precise pion electroproduction experiments and theoretical calculations in lattice QCD including three dynamical flavors [12] have established the existence of quadrupole strength in the electromagnetic transition, connected to a deformation in the nucleon and/or Delta wavefunctions. Calculations of the axial-vector [13] and pseudoscalar $N - \Delta$ transition form factors [9] have addressed pion pole dominance in the $N - \Delta$ system and the validity of the associated non-diagonal GT relation.

2 Nucleon matrix elements and form factors

2.1 Electromagnetic form factors

The nucleon electromagnetic matrix element for real or virtual photons is parameterized in terms of the Dirac, F_1, and Pauli, F_2, form factors,

$$\langle\, N(p',s')\,|j_\mu|\,N(p,s)\rangle = i\,\overline{u}(p',s')\left[\gamma_\mu F_1(q^2) + \frac{i\sigma_{\mu\nu}q^\nu}{2M_N}F_2(q^2)\right]u(p,s) \quad (1)$$

where $p(s)$ and $p'(s')$ denote initial and final nucleon momentum (spin) and M_N is the nucleon mass. The form factors depend only on the momentum transfer squared, $q^2 = (p'_\mu - p_\mu)(p'^\mu - p^\mu)$. The value of the Dirac form factor at the real photon point, $F_1(0)$, is equal to the charge of the proton (neutron) while the Pauli form factor value at the origin, $F_2(0)$, measures the anomalous magnetic moment. They are connected to the electric, G_E, and magnetic, G_M, Sachs form factors by the relations

$$\begin{aligned} G_E(q^2) &= F_1(q^2) + \frac{q^2}{(2M_N)^2}F_2(q^2) \\ G_M(q^2) &= F_1(q^2) + F_2(q^2) \end{aligned} \quad (2)$$

where $G_M(0)$ measures the nucleon magnetic moment, $\mu_p = 2.79$ for the proton and $\mu_n = -1.91$ for the neutron.

The isoscalar contribution of the electromagnetic current requires the calculation of disconnected loop diagrams. Such diagrams require the evaluation of the quark propagator from *all-to-all* lattice space-time points, a notoriously difficult task given current resources. As done in all curent lattice computations on form factors we neglect disconnected contributions. Therefore we can only calculate directly the isovector transition matrix element. In the isospin limit the following equality holds

$$\langle\, p\,|(\frac{2}{3}\overline{u}\gamma^\mu u - \frac{1}{3}\overline{d}\gamma^\mu d)|p\rangle - \langle\, n|(\frac{2}{3}\overline{u}\gamma^\mu u - \frac{1}{3}\overline{d}\gamma^\mu d)|n\rangle \;= \langle\, p\,|(\overline{u}\gamma^\mu u - \overline{d}\gamma^\mu d)|p\rangle. \quad (3)$$

Calculation of the isovector matrix element therefore provides the *isovector* nucleon form factors which measure the difference of the respective proton and neutron form factors

$$\begin{aligned} G_E(q^2) &= G_E^p(q^2) - G_E^n(q^2)\,, \\ G_M(q^2) &= G_M^p(q^2) - G_M^n(q^2)\,. \end{aligned} \quad (4)$$

2.2 Axial-vector and pseudoscalar form factors

The axial vector and pseudoscalar density are defined by

$$A^a_\mu(x) = \overline{\psi}(x)\gamma_\mu\gamma_5\frac{\tau^a}{2}\psi(x) \qquad , \qquad P^a(x) = \overline{\psi}(x)\gamma_5\frac{\tau^a}{2}\psi(x) \tag{5}$$

where τ^a are the three Pauli-matrices acting in flavor space and ψ is the isospin doublet of u- and d- quarks. The matrix element of the axial vector current between nucleon states can be written in the form

$$\langle N(p',s')|A^3_\mu|N(p,s)\rangle = i\,\overline{u}(p',s')\left[\gamma_\mu\gamma_5\,G_A(q^2) + \frac{q_\mu}{2M_N}\gamma_5\,G_p(q^2)\right]\frac{\tau^3}{2}u(p,s) \tag{6}$$

where G_A is the axial vector form factor and G_p the induced pseudoscalar form factor.

The value $G_A(0)$ defines the axial vector charge of the nucleon, obtained through nucleon β-decay measurements, $g_A = G_A(0) = 1.2695(29)$.

Spontaneous breaking of chiral symmetry leads to the relation $\partial^\mu A^a_\mu = f_\pi m_\pi^2 \pi^a$ between the pion field and the axial vector current. In QCD the corresponding relation is known as the Ward-Takahashi identity $\partial^\mu A^a_\mu = 2m_q P^a$ where m_q is the averaged light flavor doublet quark mass. The pion field is therefore proportional to the pseudoscalar density, $\pi^a = 2m_q P^a / f_\pi m_\pi^2$.

Taking the nucleon matrix element of the pseudoscalar current defines the pseudoscalar (or pion - nucleon) form factor $G_{\pi NN}(q^2)$

$$2m_q < N(p',s')|P^3|N(p,s) >= \frac{f_\pi m_\pi^2\, G_{\pi NN}(q^2)}{m_\pi^2 - q^2}\,\overline{u}(p',s')i\gamma_5\frac{\tau^3}{2}u(p,s). \tag{7}$$

The value $G_{\pi NN}(0)$ defines the low energy pion nucleon strong coupling constant, $g_{\pi NN} = G_{\pi NN}(0) = 13.2(1)$ measured from low energy pion - nucleon scattering. PCAC relates the nucleon axial form factors to $G_{\pi NN}$: taking the divergence of Eq. (6) leads to

$$G_A(q^2) + \frac{q^2}{4M_N^2}G_p(q^2) = \frac{1}{2M_N}\frac{2G_{\pi NN}(q^2)f_\pi m_\pi^2}{m_\pi^2 - q^2} \quad . \tag{8}$$

The pion pole appearing in the right hand side of Eq. 8 implies a similar pole in G_p:

$$\frac{1}{2M_N}G_p(q^2) \sim \frac{2G_{\pi NN}(q^2)f_\pi}{m_\pi^2 - q^2} \quad . \tag{9}$$

Substituting the expression for G_p in Eq. (8) leads to the Goldberger-Treiman relation

$$G_{\pi NN}(q^2)\, f_\pi = M_N G_A(q^2) \quad . \tag{10}$$

Eq. (10) is satisfied for $q^2 = 0$ at the 2% level, as $g_{\pi NN}\, f_\pi = M_N\, g_A$.

3 Lattice techniques

The evaluation of the matrix elements in Eqs. (1), (6) and (7) is performed using standard techniques in Lattice QCD. Three point functions of the nucleon interpolating operators interacting with the fermionic billinear are calculated using the *sequential inversion through the sink* technique. With this technique, the nucleon source and sink operators are fixed at well separated Euclidean time slices and billinear operator insertions of arbitrary momentum can be calculated at all intermediate Euclidean time slices. We stress the importance of exploiting particular linear combinations of the source and sink fields which maximize the number of allowed lattice momenta insertions and therefore determine the form factors at maximal accuracy in a rotationally symmetric fashion [8,9]. Appropriate ratios of three point functions and nucleon two point functions are constructed, which in the limit of large Euclidean time separation between the current and the nucleon sources converge to the desired matrix element. Smeared quark fields and gauge links are utilized in order to enhance the overlap of the interpolating field to the nucleon state and minimize the contamination from excited states.

4 Results

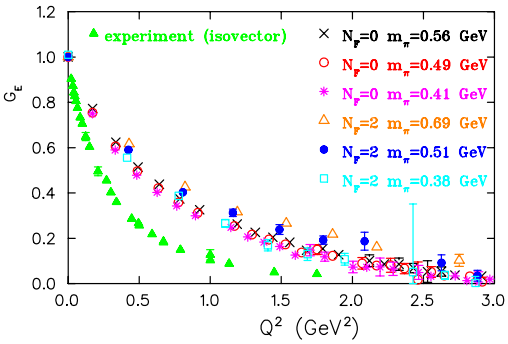

Figure 1: G_E as a function of Q^2. Filled triangles show extracted experimental results for the isovector electric form factor

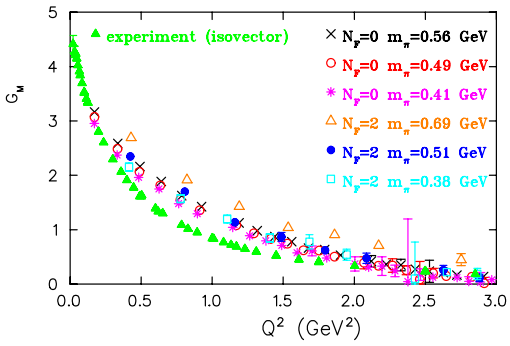

Figure 2: The isovector magnetic form factor, G_M, as a function of Q^2. The notation is the same as in Fig. 1.

An ensemble of 200 quenched ($N_F = 0$) configurations on a lattice of size $32^3 \times 64$ is utilized at three Wilson quark mass parameters corresponding to pion masses of 0.56, 0.49 and 0.41 GeV respectively. The spatial extent of 3.2 fm is large enough to ensure that finite volume effects are small. The lattice spacing obtained using the nucleon mass at the physical limit is $a = 0.09$ fm.

In addition, the study is performed on $(1.9\ \mathrm{fm})^3$ ensembles which include a dynamical doublet of light (u,d) Wilson quarks [14, 15] and corresponding pion masses of 0.69, 0.51 and 0.38 GeV.

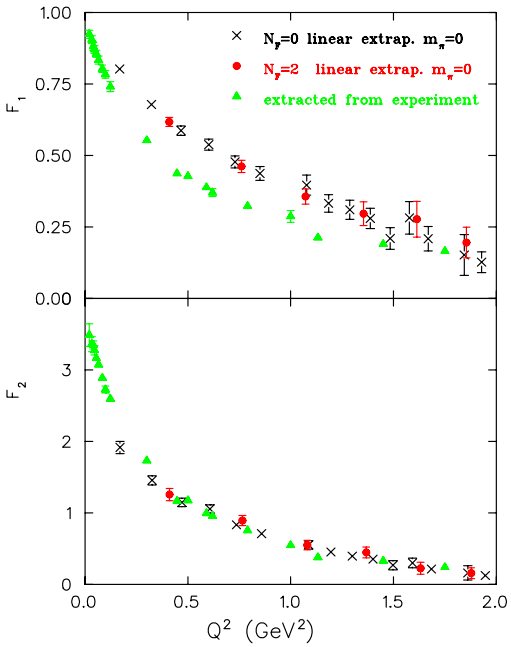

Figure 3: F_1 (upper) and F_2 (lower) as a function of Q^2 at the chiral limit. Results extracted from experiment are shown by the filled triangles.

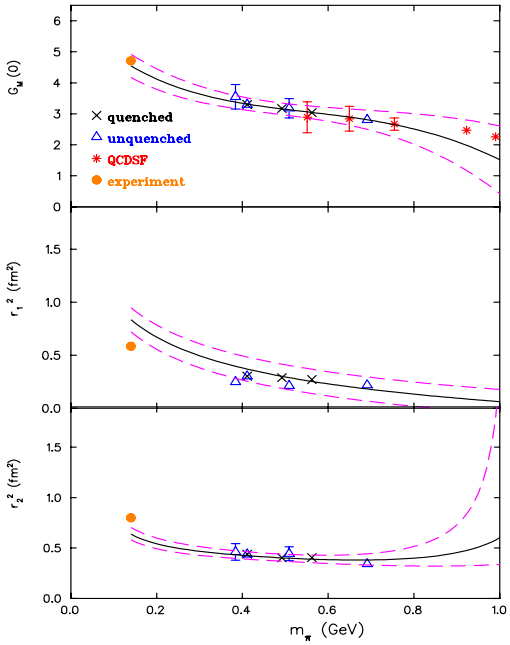

Figure 4: Chiral extrapolation of $G_M(0)$ and the rms radii r_1 and r_2. The dashed lines show the maximal error band using the errors on the fitted parameters.

In order to compare the calculated isovector form factors to experiment, we deduce the isovector part of the form factors from the available experimental data via Eqs. (4). G_E^p is well described by the dipole *Ansatz*, $G_d(Q^2) = 1/(1 + Q^2/0.71)^2$ while for the neutron the Galster parametrization is assumed

$$G_E^n(Q^2) = \frac{-\mu_n \tau}{1 + 5.6\tau} G_d(Q^2)\ , \tag{11}$$

where $Q^2 = -q^2 > 0$, $\tau = Q^2/4{M_N}^2$ and $\mu_n = -1.91$. Both G_M^p and G_M^n are interpolated to the same q^2 value using G_d. In Figures 1, 2 we show the isovector form factors for all the lattices compared to the extracted experimental isovector data. The Lattice data show a weak quark mass dependence for both G_E and G_M while unquenching effects are small. G_E shows a larger deviation to experiment than G_M. For the pion masses considered here the decreasing tendency as m_π becomes smaller is well described by a linear dependence in m_π^2. Using a linear extrapolation scheme the form factors F_1 and

F_2 are obtained at the chiral limit and shown in Fig. 3. F_2 is in agreement with experiment while F_1 clearly remains above.

Assuming a dipole Ansatz for G_E and G_M we can extrapolate to zero q^2, to extract the magnetic moment $\mu = G_M(0)$. The isovector Dirac and Pauli rms radii are related to the dipole masses M_i via

$$< r_i^2 >= -\frac{6}{F_i(Q^2)} \frac{dF_i(Q^2)}{dQ^2}|_{Q^2=0} = \frac{12}{M_i} , \quad i = 1, 2 \quad . \tag{12}$$

The dependence of μ, $< r_1^2 >$ and $< r_2^2 >$ on the pion mass has been studied within a chiral effective theory including the Δ resonance in [2]. Varying consistently the parameters in the expressions we obtain the results shown in Fig. 4. Quenched and dynamical data for μ are well described by the effective theory and extrapolate nonlinearly to the physical value. The Dirac radii on the other hand miss the physical value as expected from the fact that F_1 is decreasing slower than experiment in the low Q^2 regime.

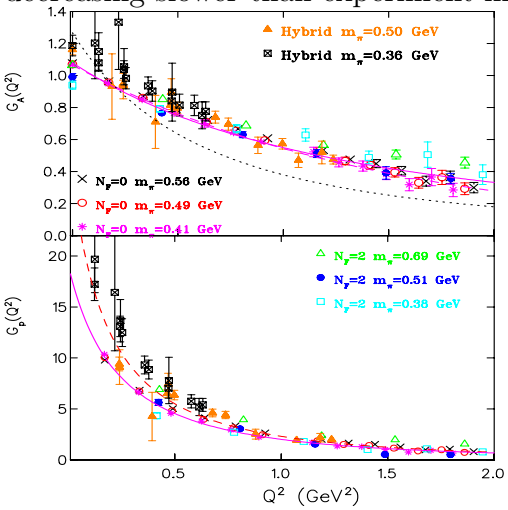

Figure 5: $G_A(Q^2)$ (upper) and $G_p(Q^2)$ (lower) for the Wilson lattices. Hybrid results are taken from Hägler *et al.* [11].

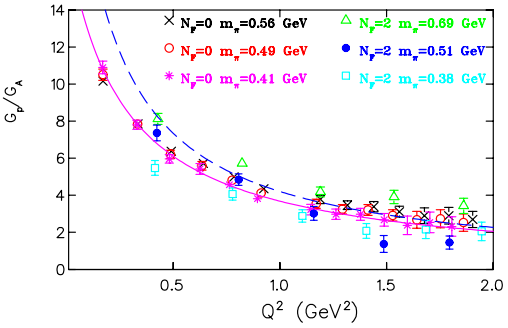

Figure 6: $G_p(Q^2)/G_A(Q^2)$ for the Wilson lattices. Pion pole dominance prediction for the 0.41 GeV pion quenched data is shown by the dashed line. The solid line is the fit to monopole form with fitted pion pole mass.

Our results for the nucleon axial form factors G_A and G_p are shown in Fig. 5. Results using MILC configurations and domain wall fermions [11] at similar pion masses are included. The dotted line in the upper plot is a fit to the experimental results taking a dipole Ansatz $G_A(q^2) = g_A / \left(1 - \frac{q^2}{M_A^2}\right)^2$, with an axial mass, $M_A = 1.026 \pm 0.0021\,\mathrm{GeV}$. The lattice results fall off slower than experiment and although described well by dipole fits, the fitted dipole masses are considerably larger than experiment. The hybrid data deviate from the Wilson data at low Q^2 and approach the expected g_A value at

the origin. G_p data are presented in the lower plot where a similar deviation between full and quenched results at low q^2 is seen. If pion pole dominance holds, the ratio $G_p(Q^2)/G_A(Q^2)$ is completely fixed from Eqs. (9), (10):

$$\frac{G_p(Q^2)}{G_A(Q^2)} = \frac{4M_N^2}{m_\pi^2 + Q^2} \ . \tag{13}$$

In Fig. 6 we show the ratio G_p/G_A together with the prediction using pion pole dominance as given in Eq. 13 for the smallest pion mass in the quenched theory (dashed line). As can be seen the lattice data show weaker q^2 depedence. Allowing the pion mass in the monopole form to vary in the fit achieves a good description of the data as shown with the solid line.

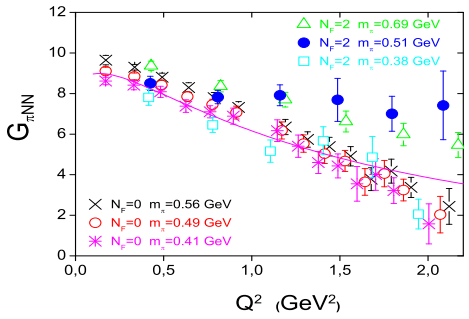

Figure 7: $G_{\pi NN}(Q^2)$ form factor for the Wilson theory quarks. The solid line is the fit of the 0.41 GeV pion data to Eq. (14).

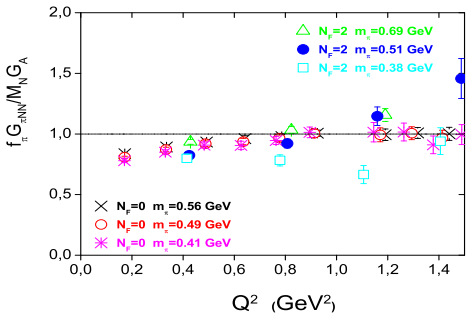

Figure 8: $f_\pi G_{\pi NN}/M_N G_A$ as a function of Q^2. If the GT relation holds exactly this ratio should be unity (solid line).

The pseudoscalar form factor $G_{\pi NN}(Q^2)$ is extracted from Eq. (7). The quark mass m_q and pion decay constant f_π which enter Eq. (7) are calculated from appropriate two point functions [9] of the axial and pseudoscalar current through the Ward-Takahashi identity $\partial^\mu A_\mu^a = 2m_q P^a$ and $\langle 0|A_\mu^a(0)|\pi^b(p)\rangle = if_\pi p_\mu \delta^{ab}$ respectively. In Fig. (7) $G_{\pi NN}(Q^2)$ is shown for all the Wilson quark lattices. These results are described well by a fit function

$$G_{\pi NN}(Q^2) = K_N \frac{Q^2/m_\pi^2 + 1}{(Q^2/m_A^2 + 1)^2 (Q^2/m^2 + 1)} \tag{14}$$

where m_A is the mass in the dipole *Ansatz* of G_A, m is the mass in the monopole fit of G_p/G_A and K_N an overall fit constant. The fit of the $m_\pi = 0.41$ GeV quenched data is shown by the solid line in Fig. (7) and the extrapolated value at $Q^2 = 0$ underestimates the experimental value. The fact that at low Q^2 the observed behavior is different than the one expected is

reflected in the plot of the $f_\pi\, G_{\pi NN}(Q^2)/M_N\, G_A(Q^2)$ ratio (Fig. 8) which is expected to be unity if the GT relation is valid. It is indeed observed that in the quenched theory this ratio is less than one for small Q^2 but becomes one for $Q^2 \gtrsim 0.5$ GeV^2. The dynamical Wilson theory shows an approximately similar behavior for the two heaviest pion masses. If on the other hand the validity of the GT relation $f_\pi G_{\pi NN} = M_N G_A$ is assumed at low Q^2, the lightest pion data in the quenched theory extrapolate to $g_{\pi NN} = 11.8 \pm 0.3$, closer to the experimentally extracted 13.2(1) value.

5 Conclusions

Rapid progress in Lattice QCD has recently allowed calculations of nucleon structure in the pion mass regime where chiral effective theory is applicable allowing reliable extrapolations to the chiral limit. We have calculated the isovector electromagnetic, axial and pseudoscalar form factors of the nucleon with optimal techinques in a wide range of momenta transfers and pion masses down to 380 MeV in the Wilson theory. Assuming that finite spacing effects are under control, the linear extrapolation of F_1 and F_2 to the chiral limit shows small unquenching effects and results to higher values for F_1 compared to experiment. The magnetic moment data extrapolate to the physical value via the one loop chiral effective theory prediction. The isovector radii are underestimated as F_1 and F_2 incease slower than experiment at low Q^2, a result of truncated pion cloud effects at the heavy quark mass lattice simulations. The importance of chiral symmetry breaking and the associated pion pole dominance in the axial vector transition is also studied. It is observed that G_p/G_A is described by a monopole form with a pole mass heavier than the corresponding pion mass. G_A is well described by a dipole *Ansatz*, in agreement to experiment, *albeit* requiring dipole masses $\gtrsim 1.5$ GeV as compared to $m_A \sim 1.1$ GeV observed in experiment. Large unquenching effects are observed for both G_A and G_p when we compare to the 350 MeV pion mass hybrid lattices [11] confirming expectations for the importance of pion cloud effects at low Q^2. The pseudoscalar form factor $G_{\pi NN}$ also increases less rapidly than the expected from the Goldberger-Treiman relation dipole form at low Q^2. This results to an underestimation of the strong coupling constant $g_{\pi NN}$ as compared to experiment. We plan to further investigate the behavior of this quantity using different lattice discretization schemes for fermions in order to check lattice cut off effects while approaching lighter pion masses.

Acknowledgments

I am indebted to C. Alexandrou, G. Koutsou, Th. Leontiou and J. W. Negele for the very enjoyable and fruitful collaboration on the topics covered in this talk. The authors of [14,15] are acknowledged for providing the unquenched configurations used in this work. I acknowledge support by the University of Cyprus and the program "Pythagoras" of the Greek Ministry of Education. Computer resources were provided by NERSC under contract No. DE-AC03-76SF00098.

References

[1] M. Jones, *et al.*, *Phys. Rev. Lett.* **84**, 1398 (2000); O. Gayou, *et al.*, *Phys. Rev.* **C64**, 038202 (2001); O. Gayou *et al.*, *Phys. Rev. Lett.* **88**, 092301 (2002).

[2] M. Gockeler *et al.*, [QCDSF Collab.] *Phys. Rev.* **D71**, 034508 (2005).

[3] T. R. Hemmert and W. Weise, *Eur. Phys. J.* **A15**, 487 (2002).

[4] A. L. Ahrens *et al.*, *Phys. Lett.* **B202**, 284 (1988).

[5] V. Bernard, N. Kaiser and U.-G. Meissner, *Phys. Rev. Lett.* **69**, 1877 (1992).

[6] S. Choi *et al.*, *Phys. Rev. Lett.* **71**, 3927 (1993).

[7] T. Gorringe and H. W. Fearing, *Rev. Mod. Phys.* **76**, 31 (2004).

[8] C. Alexandrou, G. Koutsou, J. W. Negele and A. Tsapalis, *Phys. Rev.* **D74** 034508 (2006); C. Alexandrou, hep-lat/0608025.

[9] C. Alexandrou *et al.*, *Phys. Rev.* **D76** 094511 (2007) ; C. Alexandrou *et al.*, *PoS(LATTICE2007) 162*, 2007.

[10] M. Gockeler *et al.*, [UKQCDSF Collab.] *PoS(LATTICE2007) 161*, 2007.

[11] Ph. Hägler *et al.*, arXiv:0705.4295 ; D. Richards, arXiv: 0711.2048.

[12] C. Alexandrou *et al.*, *Phys. Rev. Lett.* **94**, 021601 (2005) ; C. Alexandrou *et al.*, *Phys. Rev.* **D69**, 114506 (2004) ; C. Alexandrou *et al.*, arXiv: 0710.4621 (2007).

[13] C. Alexandrou, Th. Leontiou, J. W. Negele and A. Tsapalis, *Phys. Rev. Lett.* **98**, 052003 (2006) ; C. Alexandrou, arXiv:0710.1202 (2007); C. Alexandrou *et al.*, *PoS(LAT2006) 115*, 2006.

[14] B. Orth, Th. Lippert and K. Schilling [TχL Collaboration], *Phys. Rev.* **D72**, 014503 (2005); Th. Lippert *et al.*, *Nucl. Phys. Proc. Suppl.***60A**, 311 (1998).

[15] C.Urbach *et al.*, *Comput. Phys. Commun.* **174**, 87(2006).